Scilight

Journal of Photonic Materials

https://www.sciltp.com/journals/jpm

Article

Unlocking the Secrets of Han Blue: The Art and Science behind Its Synthesis

Giorgio Enrico Gagliardo Briuccia [1], Alessandro Lo Bianco [2], Francesco Armetta [1,3], Vitalii Boiko [4,5], Dariusz Hreniak [4] and Maria Luisa Saladino [1,3,*]

[1] Department of Biological, Chemical and Pharmaceutical Sciences and Technologies (STEBICEF), University of Palermo, Viale delle Scienze, Bld.17, 90128 Palermo, Italy
[2] Department of Physic and Chemistry "E. Segrè", University of Palermo, Viale delle Scienze, Bld.17, 90128 Palermo, Italy
[3] Consiglio Nazionale delle Ricerche, Istituto per i Processi Chimico Fisici IPCF-Messina, Viale Ferdinando Stagno d'Alcontres 37, 98158 Messina, Italy
[4] Institute of Low Temperature and Structure Research, Polish Academy of Sciences, ul Okólna 2, 50-422 Wrocław, Poland
[5] Department of Physics of Biological Systems, Institute of Physics, National Academy of Sciences of Ukraine, Prospekt Nauky, 46, UA-03028, Kyiv, Ukraine

* Correspondence: marialuisa.saladino@unipa.it

How To Cite: Gagliardo Briuccia, G.E.; Lo Bianco, A; Armetta, F.; et al. Unlocking the Secrets of Han Blue: the Art and Science behind Its Synthesis. *Journal of Photonic Materials* **2025**, *1*(1), 100001.

Received: 4 January 2025
Revised: 6 February 2025
Accepted: 8 April 2025
Published: 5 September 2025

Abstract: *Han Blue* (HB, $BaCuSi_4O_{10}$) is a historically significant pigment widely used in ancient Chinese art and artifacts, recently found also to be able to efficiently convert red radiation into infrared radiation. This article focuses on the synthesis of Han Blue, on the one hand using what we know about ancient production techniques from the Han Dynasty, while on the other hand, through the use of modern techniques, allowing us to obtain a high-purity material that can also find use in modern optical applications. The synthesis was carried out using the solid-state synthesis method, particularly focusing on the effect of temperature treatment on the final physicochemical properties of the obtained samples. Results are showing that the temperature affects the composition of the powders. It has also been shown that under certain conditions of Han Blue synthesis, it is also possible to obtain varying amounts of the side phase of the so-called *Purple Han*, another synthetic pigment also used in ancient China, characterized by different optical properties.

Keywords: infrared emission; Han Blue; Purple Han; solid state method

1. Introduction

Han Blue (HB) [1], also known as Chinese Blue, is an ancient material with a history that dates back to ancient China [2]. Like its counterpart, Egyptian Blue (EB) [1], HB has intriguing features and has been employed as a pigment in antiquity. The main constituent of HB is a two-layered barium and copper silicate, $BaCuSi_4O_{10}$, which shares a structural similarity with $CaCuSi_4O_{10}$ found in EB, differing only in the presence of Ba^{2+} instead of Ca^{2+} [3]. Despite these similarities, it's noteworthy that HB was developed in China more than 2000 years later than EB, suggesting an independent historical evolution [4,5]. Additionally, rare natural analogous of HB's main constituents have been discovered in Kalahari Manganese Field, South Africa, named "Effenbergerite" [6]. Initially, it was linked to the Han Dynasty due to its discovery in archaeological findings from that period (206 BCE–220 CE) [7]. However, more recent research revealed that Chinese Blue was in use long before the Han Dynasty [8]. HB shares with EB intriguing photoluminescent properties, particularly in the Near Infrared Region (NIR). What sets HB apart is its unique photoluminescent behaviour, notably associated with the electronic transition $^2B_{2g} \rightarrow {}^2B_{1g}$ [9]. This transition leads to emission wavelengths ranging between 900 and 1000 nm. What's fascinating is the variety of excitation sources that can induce this luminescence, including visible light in

the red and green regions, absorptions in the NIR-I region at around 780 nm [10], and UV light [11]. The photoluminescence of Han Blue is radiative and mainly attributed to Cu^{2+} ions located within its crystal lattice. These ions, situated on a fourfold axis and in square planar coordination, are linked to four SiO_4 tetrahedra. This unique arrangement of Cu^{2+} ions in Han Blue is the key to its distinctive photoluminescent properties [12]. Han Blue's photoluminescence is usually used to identify and map the distribution of the pigment through multispectral imaging methods, such as Visible Induced Luminescence imaging (VIL) [13,14]. VIL has become an indispensable tool in Conservation Science, enabling researchers to explore the secrets of this ancient pigment in archaeological sites and conservation institutions. In addition to the knowledge about its emission in the IR region, the HB is also under investigation for more modern applications such as silica-based optical amplifiers, security ink, laser technology [15] and it is widely used in biomedical analysis, archaeological imaging and optical sensors [16].

There is no single ancient Chinese manuscript that explicitly transmits the recipe for HB. However, HB has been discovered on ceramic artifacts, murals, and funerary decorations. Objects recovered from high-ranking tombs of the Han dynasty are the main sources of knowledge. The details of its composition and production method have been reconstructed through chemical and archaeological studies. Modern experiments have replicated the pigment to understand the original processes [1]. However, the solid reaction is usually not enought to obtain pure products [17,18]. Pure HB and Han Purple (HP) can be obtained combining coprecipitation an hydrothermal method followed by the thermal treatment [16]. However, in archaeological artifacts, HB is often found in contamination with HP. This phenomenon is well-documented and occurs primarily because the two pigments share similar chemical compositions and were often produced within the same technological context. Both pigments are synthetic silicates, with HB being a barium copper silicate ($BaCuSi_4O_{10}$), while HP is a slightly different barium copper silicate ($BaCuSi_2O_6$). The structural similarity implies that their synthesis could produce traces of one pigment as a byproduct of the other. During high-temperature synthesis (around 850–1000 °C), variations in the proportions of the starting materials (copper, barium, silica) could lead to the formation of both blue and purple pigments. Ancient workshops did not have precise control over chemical conditions as we do today, so natural contamination between the pigments occurred. In recovered ancient artifacts, such as murals and ceramics, HB and HP are often found mixed, likely because they were used in close proximity or because the blue pigment was altered during the fabrication or application process.

In addition, recently some authors highlighted the use of HB for novel modern applications such as detection of latent fingermarks [19], optical sensing materials [20], and smart inks, energy storage, bioimaging, and phototherapy [21,22]. On the other hand, in some cases the HB available in the market, is not a pure HB, but is proposed to be used for some particular applications. Thus, the knowledge of the effect of synthesis parameters and how to control the product features is important on the light of the above applications. So that, the goal of this work was to synthesize HB in order to evaluate its composition depending of the temperature of calcination. To do this, the traditional procedure of synthesis by solid state method has been used, while employing the modern technologies [23]. By investigating the effect of the temperature of calcination, we aim to understand the structural evolution of the pigment.

The investigation of structure and morphology of the obtained powders was performed by X-ray diffraction and FT-IR Spectroscopy. The visible induced luminescence (VIL) was used to preliminary investigate the optical properties, observing the emission in the NIR range after using a red LED lamp (centred at 640 nm) as light source. The luminescence properties were determined by luminescence spectroscopy (emission (PL) and excitation (PLE) spectra and decay time measurements). The color coordinates have been also calculated.

2. Material and Methods

2.1. List of Reagents

Copper(II) carbonate hydroxide $Cu_2CO_3(OH)_2$ (Sigma-Aldrich (St. Louis, MO, USA), reagent grade CAS 12069-69-1), Barium Carbonate $BaCO_3$ (ACS reagent, ≥ 99.0% CAS 513-77-9), SiO_2 Silica gel (Sigma-Aldrich high purity grade CAS 112926-00-8), Han Blue (Kremer-Pigmente GmbH & Co. KG, Germany, cod. 10071 0–40 µ, COMM-HB), Han-Purple (Kremer-Pigmente GmbH & Co. KG, Germany, cod. 10075, 40–80 µ, COMM-HP).

2.2. Synthesis of HB

The synthesis of the Han Blue (HB) samples was carried out by using the solid- state method. The stoichiometric ratios used for the synthesis are those precisely required for $BaCuSi_4O_{10}$, using $BaCO_3$, $Cu_2CO_3(OH)_2$, and silica gel as precursors [24]. 0.363 g of $BaCO_3$, 0.200 g of $Cu_2CO_3(OH)_2$, and 0.436 g of silica gel were weighted, mixed and grounded in an agate mortar. The resulting powder was thus thermally treated at

950 °C for different time in a GEFRAN 1001 ME320 muffle furnace. The five different pigments HB-1, HB-6, HB-12, HB-24, HB-48 have been obtained calcinating for 1 h, 6, 12, 24 and 48 h, respectively.

2.3. Methods and Instrumentations

Multispectral Imaging. Photos of in the visible and infrared regions were acquired illuminating the samples with a UV lamp or a 640 nm lamp, to obtain visible and infrared images, respectively, and using a 20.3 MPX NX3300 Samsung camera equipped with a manual UV-IR lens and a visible filter and an 850 nm filter for IR imaging with NEEWER filters.

XRD patterns were acquired by a Philips X'Pert PRO diffractometer (now part of Malvern PANAlytical, Malvern, UK) equipped with a fast detector (X'Celerator) using Cu-kα radiation (λ = 1.5405 Å) and operating at 40 kV and 40 mA. Each measurement was performed at room temperature in the 5–80° 2θ range with a step of 0.008° and a time for step of 5 s. The phase identification was performed by using the X'pert HighScore Plus® Software v5.3. In order to obtain information about the phase composition, the cell parameters and the crystallite size of the phases, the XRD patterns were analysed according to the Rietveld method. The agreement between the experimental data and the fit was evaluated through the curve of residues and the parameters R_{wp} (<6%), and R_b (<5%).

Reflectance spectra were acquired using an Ocean Optics USB 2000 + XR1 portable spectrometer consisting of an XR grating operating in the spectral range between 350–1000 nm, with an optical resolution of 1.7–2.1 nm (FWHM). The high-intensity UV-Vis-NIR source *Ocean Optics DH-mini* (Gernamy) consists of two deuterium and tungsten-halogen lamps, and the reflection probe is of the R400-7—UV/VIS type. Spectra were acquired with the following parameters: integration time: 5 s, scans to average: 4, boxcar width: 5. Data analysis was performed using OceanView software 2.0.8. The tool is able to provide both reflectance curves and colorimetric coordinates. The latter were acquired by setting a CIE D65 standard illuminant, a CIE 10 stardardimetric observer and the CIE *L*a*b** colour space as the reference system. The values of L*, a* and b* were derived from the reflectance spectra by processing the experimental data using OceanView software 2.0.8.

Scanning electron microscope (SEM). SEM micrographs were acquired using an FEI Company, Hillsboro, OR Quanta 200 scanning electron microscope (SEM) instrument coupled with an energy dispersion detector (EDS) for elemental analysis. The samples were fixed on an aluminum substrate using double-sided conductive carbon tape and were observed without metallization process.

Photoluminescence emission (PL) and excitation (PLE) spectra were measured using the FLS980 Fluorescence Spectrometer from Edinburgh Instruments (Livingston, UK). The 450 W Xenon lamp for both PL and PLE were used as an excitation source. The R928P side window photomultiplier tube from Hamamatsu was used as a detector. The excitation arm was supplied with a holographic grating of 1800 lines/mm, blazed at 300 nm, while the emission arm was supplied with ruled grating, 1800 lines/mm blazed at 500 nm in Czerny Turner configuration. The scanning range was from 250 nm to 850 nm for PLE spectra and from 750 nm to 1200 nm for PL spectra. All spectra were corrected for the sensitivity of the detection channel (PL) and the intensity of incident radiation (PLE).

The *lifetime measurements* were carried out using the same instrument while a 150 W Xe pulsed lamp was used as the excitation source. A mono-exponential decay curve as described in Equation (1) was fitted to the decay curves.

$$I(t) = I_0 + e^{(-(t-\tau_0)/t_1)} + I_{offset} \quad (1)$$

3. Results and Discussion

All obtained powders are showing the characteristic emission in the IR region (Figure 1).

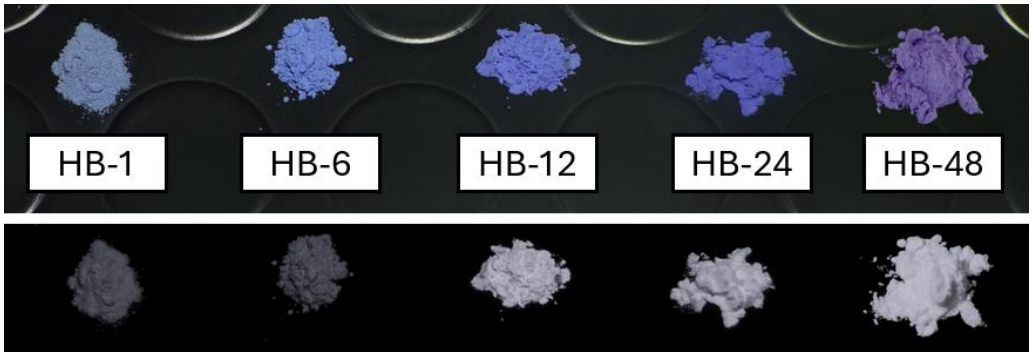

Figure 1. Photos of HB powders in VIS range (**up**) and NIR emission after irradiation by a 640 nm red LED lamp (**down**).

The powders were characterized by acquiring the X-ray diffraction (XRD).

From the phase analysis carried out on the XRD patterns (Figure 2, up), the presence of the $BaCuSi_4O_{10}$ phase, known as *Effenbergerite*, the HB know phase, was confirmed in all the samples. However, in the HB-1 and HB-6 powders, the $BaCuSi_2O_6$, known as *Colinowensite*, $BaCu_2Si_2O_7$, known as *Scottyite* [25], and $BaSiO_3$ are present. After 12, 24 and 48 h of treatment, only *Colinowensite* $BaCuSi_2O_6$ [26] is present together with effenbergerite. The *Colinowensite* is the mineral constituting the Han Purple (HP), which amount is increasing with the treatment time (Table 1). These two phases are present also in two commercial HB and HP powders (Figure 2, down).

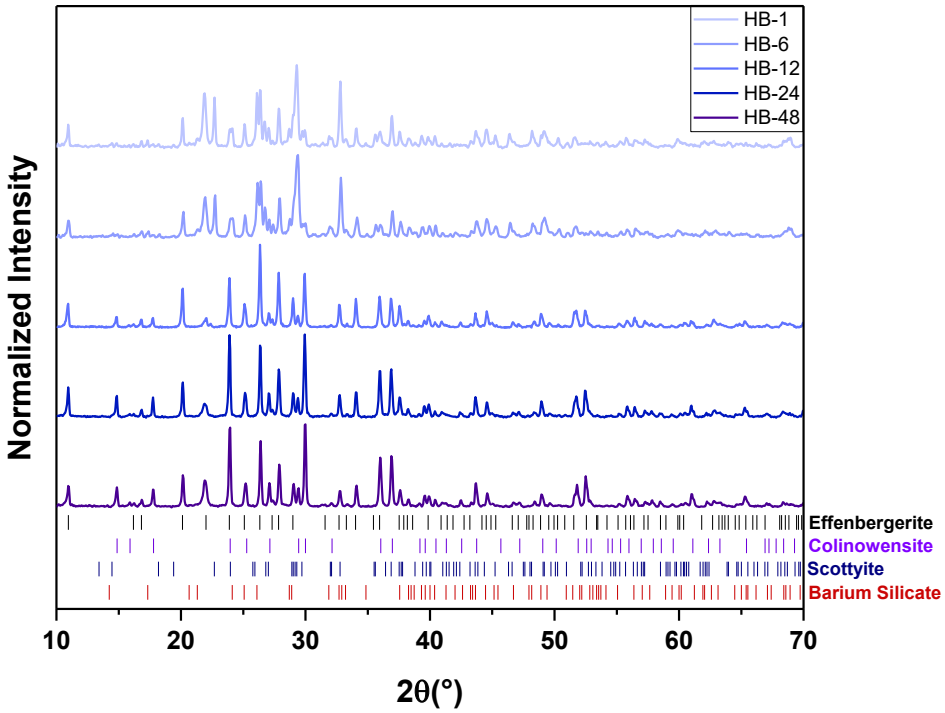

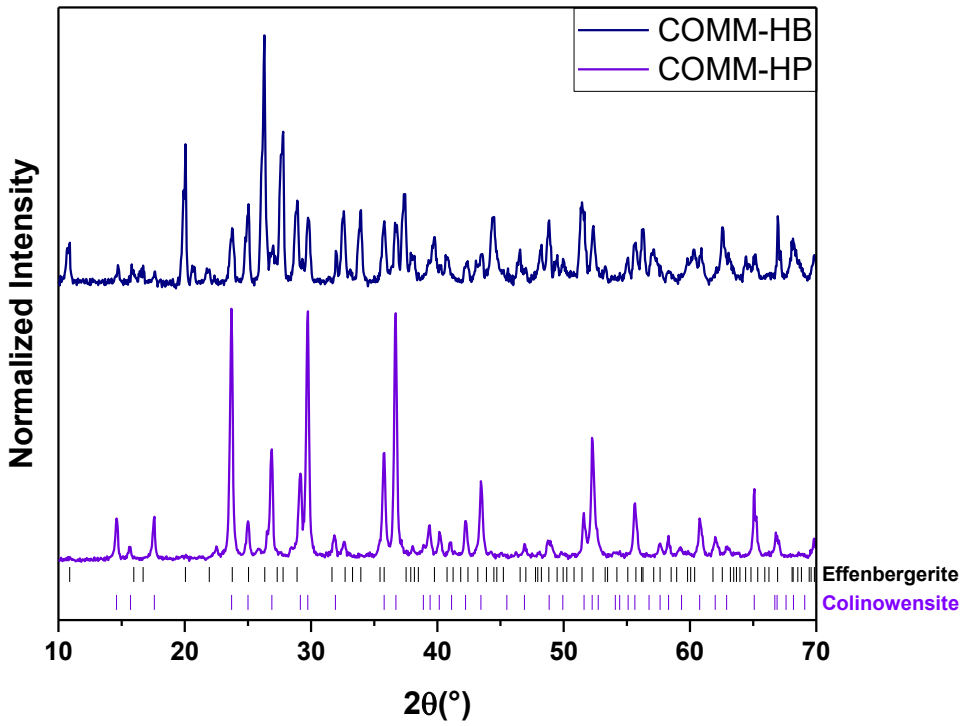

Figure 2. XRD patterns of HB-1, HB-6, HB-12, HB-24 and HB-48 powders with reference phases and of the commercial powders.

Table 1. Phase composition HB-1, HB-6, HB-12, HB-24, HB-48 powders and of two commercial HB and HP powders. $BaCuSi_4O_{10}$ is Efferbengerite and $BaCuSi_2O_6$ is Colinowensite. The blue and purple color of the phase is an indication of the pigment color.

Samples	Phases	$\%_{w/w}$
HB-1	$BaCuSi_4O_{10}$	32
	$BaCu_2Si_2O_7$	38
	$BaCuSi_2O_6$	12
	$BaSiO_3$	18
HB-6	$BaCuSi_4O_{10}$	34
	$BaCu_2Si_2O_7$	36
	$BaCuSi_2O_6$	13
	$BaSiO_3$	17
HB-12	$BaCuSi_4O_{10}$	50
	$BaCuSi_2O_6$	50
HB-24	$BaCuSi_4O_{10}$	52
	$BaCuSi_2O_6$	48
HB-48	$BaCuSi_4O_{10}$	36
	$BaCuSi_2O_6$	64
COMM-HB	$BaCuSi_4O_{10}$	86
	$BaCuSi_2O_6$	14
COMM-HP	$BaCuSi_4O_{10}$	28
	$BaCuSi_2O_6$	72

Since the composition of HB-24 is the most closed to the HB commercial references, the morphology and the optical properties were investigated only for this powder. The morphology, observed through SEM, of the powders is reported in Figure 3a. As we can see, the particle shape is irregular and the average particle size is around 13 μm (Figure 3b).

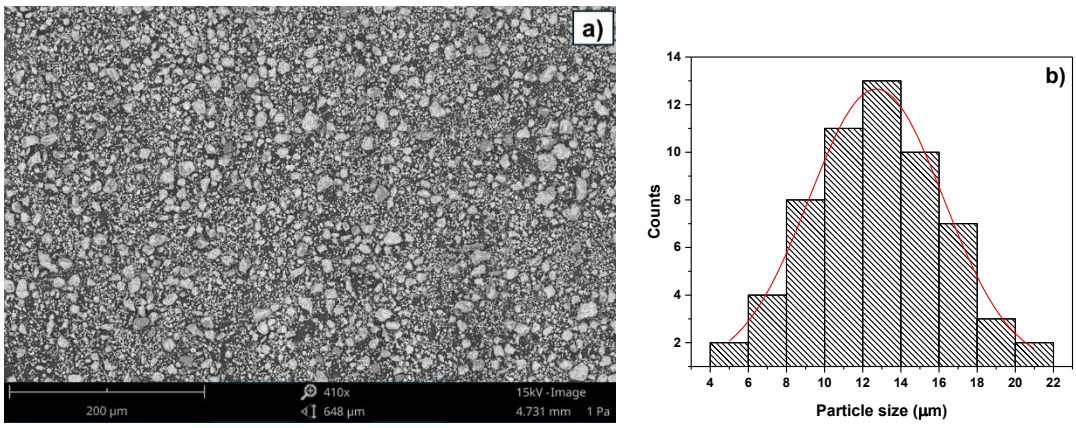

Figure 3. SEM micrograph of HB-24 (**a**) and distribution of particle size (**b**).

The reflectance spectrum of the HB-24 is shown in Figure 4a. As you can see, the UV-vis reflectance spectra profile is very similar to the one of the commercial Han blue. The CIE_{Lab} graph, reported in Figure 4b, shows that the color coordinates of the powder are located in the blue region of the chart. However, there are a few small differences with the commercial samples, reflecting the color coordinates (Figure 3b), probably due to the bigger particle size, 40 µm in average.

The excitation spectra (Figure 5a) of the HB-12, HB-24 and H-48 powders show the presence of four bands: the charge transfer band (CTB) at approximately 250 nm, the band related to the $^2B_{1g} \rightarrow {}^2A_{1g}$ transition at around 550 nm, the main band associated with the $^2B_{1g} \rightarrow {}^2E_g$ transition at about 628 nm, and the band related to the $^2B_{1g} \rightarrow {}^2B_{2g}$ transition at approximately 780 nm [9]. The presence of these bands in the Han Blue excitation spectrum can be attributed to the fact that the crystal structure of effenbergerite belongs to the gillespite group ($BaFeSi_4O_{10}$) with a tetragonal crystal system and space group *P4/ncc*, which is the same as that of cuprorivaite [27,28]. Therefore, the Cu^{2+} ion has the same coordination environment, with a square planar structure, from which the aforementioned bands originate [9]. The emission spectrum (Figure 5b) shows a band centred at ~950 nm, which is also related to the $^2B_{2g} \rightarrow {}^2B_{1g}$ transition. As we can see, despite a small shift in the excitation band centred at 628 nm of HB-24, no large differences can be observed in all spectra. On the other hand, the luminescence decay profiles and the lifetimes of the of HB-12, HB-24 and H-48 samples, reported in Figure 6, are in line with the literature-reported range of 100–150 µs [21].

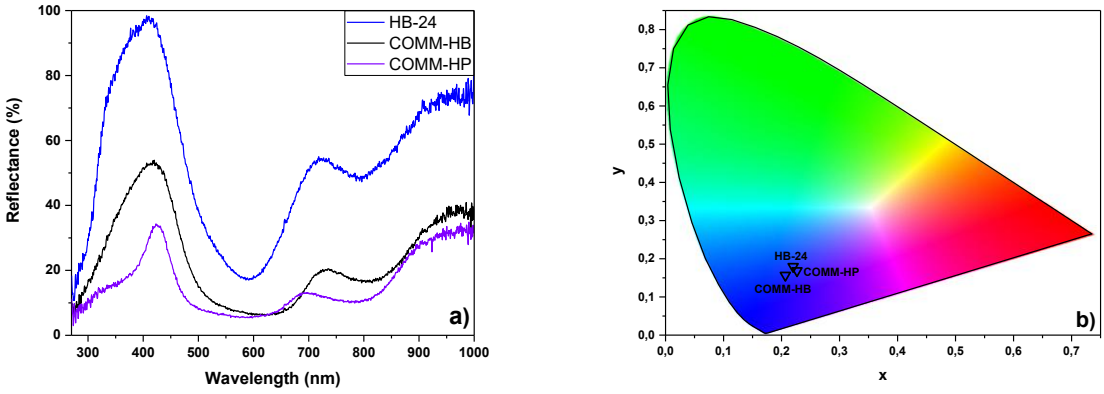

Figure 4. Reflectance spectra (**a**) and color coordinates (**b**) of HB-24 and of commercial samples.

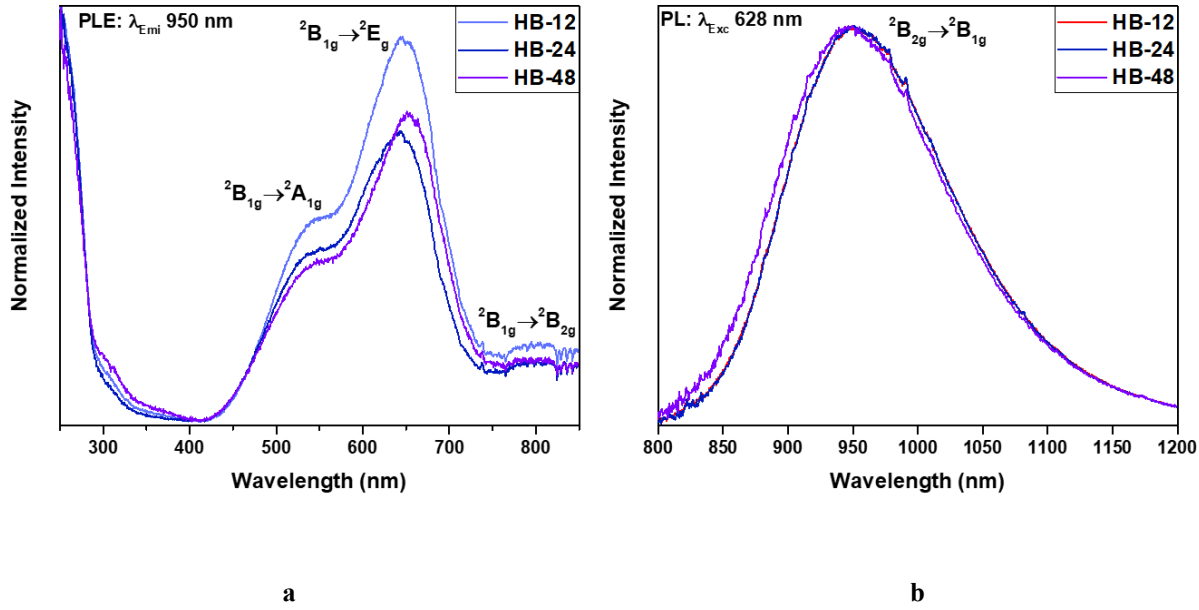

Figure 5. Excitation spectra at λ_{Emi} 950 nm (**a**) and emission spectra at λ_{Exc} 628 nm (**b**) of HB-12, HB-24 and H-48 powders.

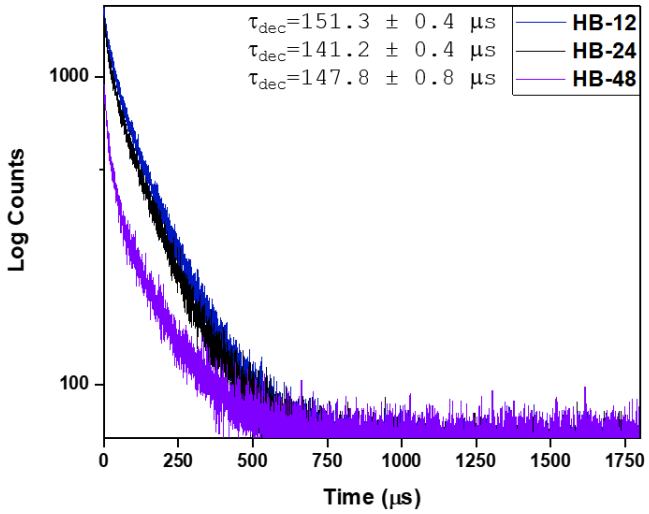

Figure 6. Decay time profile of HB-12, HB-24 and H-48 powders.

4. Conclusions

The goal of this study was to understand how the synthesis of Han Blue was influenced by the calcination time. The HB pigment was synthesized by a solid state method followed by a calcination at 950 °C. The results showed that the powder composition is affected by the temperature and that the composition of powder treated at 24 h is the closest to the commercial Han Blue. In this condition, the particle shape is irregular with the average size of 13 µm Both the color coordinates that the optical properties are the one related to the HB. However, it is necessary to underline that the Han Blue pigment is constituted also by the Purple Han, a synthetic pigment used in ancient China alongside the closely related Han Blue and the optical properties are affected by the powder composition.

The findings contribute to the broader field of heritage science by facilitating the creation of authentic replicas for conservation purposes and offering insights into ancient manufacturing technologies. This research bridges historical craftsmanship with contemporary material science, highlighting the enduring significance of Han Blue in art and technology.

Author Contributions

M.L.S. and D.H.: Conceptualization and methodology, writing—review and editing. G.E.G.B and ALB.: Synthesis and Preparations, XRD patterns, color coordinates. F.A.: SEM investigation. V.B. and D.H.: optical properties (PL and PLE spectra, decay times). All authors have read and agreed to the published version of the manuscript.

Funding

F.A. thanks MIUR for the Project PON Ricerca e Innovazione 2014–2020–Avviso DD 407/2018 "AIM Attrazione e Mobilità Internazionale" (AIM1808223). GEGB and ALB thanks the University of Palermo for supporting his research work through the progetto "Viaggi e soggiorni di studio degli studenti" A.A. 2022–2023 and 2023–2024, respectively.

Data Availability Statement

The datasets generated during and/or analysed during the current study are available from the corresponding author on reasonable request.

Acknowledgments

M.L.S. and D.H. thank the University of Palermo for the CORI2023—Action C Project and FFR2024 to have the possibility of visits between the two Institutions.

Conflicts of Interest

No conflict of Interest.

References

1. Nicola, M.; Gobetto, R.; Masic, A. Egyptian Blue, Chinese Blue, and Related Two-Dimensional Silicates: From Antiquity to Future Technologies. Part A: General Properties and Historical Uses. *Rend. Fis. Acc. Lincei* **2023**, *34*, 369–413. https://doi.org/10.1007/s12210-023-01153-5.
2. Zhang, Z.; Ma, Q.; Berke, H. Man-Made Blue and Purple Barium Copper Silicate Pigments and the Pabstite ($BaSnSi_3O_9$) Mystery of Ancient Chinese Wall Paintings from Luoyang. *Herit. Sci.* **2019**, *7*, 97. https://doi.org/10.1186/s40494-019-0340-4.
3. Wiedemann, H.-G.; Berke, H. Chemical and Physical Investigations of Egyptian and Chinese Blue and Purple. 2015. Available online: http://nbn-resolving.de/urn:nbn:de:bsz:16-monstites-223513 (accessed on 11 April 2025).
4. Qin, Y.; Wang, Y.-H.; Chen, X.; et al. A Discussion on the Emergence and Development of Ancient Chinese Artificial Barium Copper Silicate Pigments from Simulation Experiments. *Archaeometry* **2016**, *58*, 796–806. https://doi.org/10.1111/arcm.12205.
5. Berke, H. The Invention of Blue and Purple Pigments in Ancient Times. *Chem. Soc. Rev.* **2007**, *36*, 15–30. https://doi.org/10.1039/B606268G.
6. Giester, G.; Rieck, B. Effenbergerite, $BaCu[Si_4O_{10}]$, a New Mineral from the Kalahari Manganese Field, South Africa: Description and Crystal Structure. *Mineral. Mag.* **1994**, *58*, 663–670. https://doi.org/10.1180/minmag.1994.058.393.17.
7. FitzHugh, E.W.; Zycherman, L.A. A Purple Barium Copper Silicate Pigment from Early China. *Stud. Conserv.* **1992**, *37*, 145–154. https://doi.org/10.1179/sic.1992.37.3.145.
8. Ma, Q.; Portmann, A.; Wild, F.; et al. Raman and SEM Studies of Man-Made Barium Copper Silicate Pigments in Ancient Chinese Artifacts. *Stud. Conserv.* **2006**, *51*, 81–98. https://doi.org/10.1179/sic.2006.51.2.81.
9. Li, Y.-J.; Ye, S.; Wang, C.-H.; et al. Temperature-Dependent near-Infrared Emission of Highly Concentrated Cu^{2+} in $CaCuSi_4O_{10}$ Phosphor. *J. Mater. Chem. C* **2014**, *2*, 10395–10402. https://doi.org/10.1039/C4TC01966K.
10. King, R.S.P.; Hallett, P.M.; Foster, D. NIR−NIR Fluorescence: A New Genre of Fingermark Visualisation Techniques. *Forensic Sci. Int.* **2016**, *262*, e28–e33. https://doi.org/10.1016/j.forsciint.2016.03.037.
11. Binet, L.; Lizion, J.; Bertaina, S.; et al. Magnetic and New Optical Properties in the UV–Visible Range of the Egyptian Blue Pigment Cuprorivaite $CaCuSi_4O_{10}$. *J. Phys. Chem. C* **2021**, *125*, 25189–25196. https://doi.org/10.1021/acs.jpcc.1c06060.
12. Pozza, G.; Ajò, D.; Chiari, G.; et al. Photoluminescence of the Inorganic Pigments Egyptian Blue, Han Blue and Han Purple. *J. Cult. Herit.* **2000**, *1*, 393–398. https://doi.org/10.1016/S1296-2074(00)01095-5.
13. Verri, G. The Spatially Resolved Characterisation of Egyptian Blue, Han Blue and Han Purple by Photo-Induced Luminescence Digital Imaging. *Anal. Bioanal. Chem.* **2009**, *394*, 1011–1021. https://doi.org/10.1007/s00216-009-2693-0.
14. Dyer, J.; Verri, G.; Cupitt, J. Multispectral Imaging in Reflectance and Photo-Induced Luminscence Modes: A User Manual. Available online: https://www.researchgate.net/profile/Giovanni-Verri-2/publication/267266175_Multispe

ctral_Imaging_in_Reflectance_and_Photo-induced_Luminescence_modes_A_User_Manual/links/5448e7560cf2d62c3052d2b7/Multispectral-Imaging-in-Reflectance-and-Photo-induced-Luminescence-modes-A-User-Manual.pdf (accessed on 11 April 2025).

15. Chen, Y.; Shang, M.; Wu, X.; et al. Hydrothermal synthesis, hierarchical structures and properties of blue pigments $SrCuSi_4O_{10}$ and $BaCuSi_4O_{10}$. *CrystEngComm* **2014**, *16*, 5418–5423. https://doi.org/10.1039/C3CE42394H.
16. Zhang, C.; Zhang, N.; Wang, X.; et al. Novel preparation of an ancient ceramic pigment $BaCuSi_4O_{10}$ and its performance investigation. *Mater. Res. Bull.* **2018**, *101*, 334–339. https://doi.org/10.1016/j.materresbull.2018.02.002.
17. Berdahl, P.; Boocock, S.K.; Chan, G.C.Y.; et al. High quantum yield of the Egyptian blue family of infrared phosphors ($MCuSi_4O_{10}$, M = Ca, Sr, Ba). *J. Appl. Phys.* **2018**, *123*, 193103. https://doi.org/10.1063/1.5019808.
18. Chen, W.; Shi, Y.; Chen, Z.; et al. Near-Infrared Emission and Photon Energy Upconversion of Two-Dimensional Copper Silicates. *J. Phys. Chem. C* **2015**, *119*, 20571−20577. https://doi.org/10.1021/acs.jpcc.5b04819.
19. La Rocca, R.; Pitman, R.; Shahbazi, S.; et al. Preliminary investigations into the use of the ancient pigments Han blue and Han purple as luminescent dusting powders for the detection of latent fingermarks Forensic Science International **2024**, *362*, 112172. doi.org/10.1016/j.forsciint.2024.112172.
20. Borisov, S.M.; Würth, C.; Resch-Genger, U.; et al. New Life of Ancient Pigments: Application in High Performance Optical Sensing Materials. *Anal. Chem.* **2013**, *85*, 19, 9371–9377. https://doi.org/10.1021/ac402275g.
21. Selvaggio, G.; Kruss, S. Preparation, properties and applications of near-infrared fluorescent silicate nanosheets. *Nanoscale* **2022**, *14*, 9553–9575. https://doi.org/10.1039/D2NR02967G.
22. Selvaggio, G.; Weitzel, M.; Oleksiievets, N.; et al. Photophysical properties and fluorescence lifetime imaging of exfoliated near-infrared fluorescent silicate nanosheets. *Nanoscale Adv.* **2021**, *3*, 4541–4553. https://doi.org/10.1039/D1NA00238D.
23. Armetta, F.; Lo Bianco, A.; Boiko, V.; et al. Multimodal anti-counterfeiting inks: Modern use of an ancient pigment in synergy with a persistent phosphor. *J. Mater. Chem. C* **2024**, *13*, 1188–1197. https://doi.org/10.1039/D4TC04228J.
24. McDaniel, J.; Salguero, D. Exfoliation of Egyptian Blue and Han Blue, Two Alkali Earth Copper Silicate-based Pigments. *J. Vis. Exp.* **2014**, e51686. https://doi.org/10.3791/51686.
25. Yang, H.; Downs, R.T.; Evans, S.H.; et al. Scottyite, the natural analog of synthetic $BaCu_2Si_2O_7$, a new mineral from the Wessels mine, Kalahari Manganese Fields, South Africa. *Am. Mineral.* **2013**, *98*, 478–484. https://doi.org/10.2138/am.2013.4326.
26. Rieck, B.; Pristacz, H.; Giester, G. Colinowensite, $BaCuSi_2O_6$, a new mineral from the Kalahari Manganese Field, South Africa and new data on wesselsite, $SrCuSi_4O_{10}$. *Mineral. Mag.* **2015**, *79*, 1769–1778. https://doi.org/10.1180/minmag.2015.079.7.04.
27. Skinner, B.J. Dana's System: The System of Mineralogy of James Dwight Dana and Edward Salisbury Dana. Yale University, 1837-1892. Vol. 3, Silica Materials. Revised and Enlarged by Clifford Frondel. Wiley, New York, Ed. 7, 1962. Xii + 334 Pp. Illus. $7.95. *Science* **1963**, *139*, 821. https://doi.org/10.1126/science.139.3557.821.a.
28. Kendrick, E.; Kirk, C.J.; Dann, S.E. Structure and Colour Properties in the Egyptian Blue Family, M1−xM′xCuSi4O10, as a Function of M, M′ Where M, M′=Ca, Sr and Ba. *Dye. Pigment.* **2007**, *73*, 13–18. https://doi.org/10.1016/j.dyepig.2005.10.006.